Dr. Jan Wilhelm, Dr. Štěpán Marek, Maximilian Graml

https://www.ur.de/physics/wilhelm/teaching/sose24-computational-nanoscience

Computational Nanoscience: Solution to Exercise Sheet No. 7

Exercise 7.1: Formulæ for the dipole moment

$$\mathbf{p}(t) = \int \mathrm{d}t' \alpha(t - t')\, \mathbf{E}(t')\,, \tag{1}$$

$$\mathbf{p}(t) = \int \mathrm{d}^3 r'\, \mathbf{r}'\, n(\mathbf{r}', t)\,. \tag{2}$$

(a) The incoming electric field $\mathbf{E}(t)$ is known, but the time-dependent polarizability tensor $\alpha_{ij}, i, j \in \{x, y, z\}$, in which all intricacies of the material are hidden, is unknown. The time integral takes care of the "memory" of the material, i.e. the response of the material from previous times at t' can influence the dipole moment at t.

Eq. (1) only holds as long as the electric field peak strength E_0 is sufficiently small, which is called linear response regime. For stronger electric fields, higher orders of $\mathbf{E}(t)$ have to be included, e.g.

$$\begin{aligned}\mathbf{p}(t) = &\int \mathrm{d}t' \alpha(t - t')\, \mathbf{E}(t') \\ &+ \int \mathrm{d}t'' \int \mathrm{d}t' \bar{\alpha}(t'', t', t)\mathbf{E}(t'')\mathbf{E}(t') \\ &+ O(\mathbf{E}(t)^3)\,,\end{aligned} \tag{3}$$

which will enhance the dipole moment beyond the linear order. Here, $\bar{\alpha}$ is a tensor of third order, i.e. with elements $\bar{\alpha}_{ijk},\ i, j, k \in \{x, y, z\}$.

(b) Eq. (2) includes all contributions to the dipole order of the emitted radiation as long as the electronic density $n(\mathbf{r}, t)$ is known exactly; which is formally the case for (TD-)DFT. In practice, we have to approximate the xc-functional, use a finite basis and similar numerical approaches and therefore introduce deviations from the exact dipole moment.

Radiation is well described by the dipole moment as long as we are in the far field; the multipole expansion is an expansion in r/R_0, where r is the distance to a (approximately) spherical charge distribution and R_0 is its radius.[1] Measuring the outgoing electric field close to the charge distribution would therefore make higher multipole-orders more important.

Exercise 7.2: Geometry

Geometry for 3Å distance:

[1] cf. e.g. Fließbach

```
    14

Mg              0.00000000              0.00000000              0.00000000
Mg             -2.14100000             -2.14100000              2.14100000
Mg             -2.14100000              2.14100000              2.14100000
Mg              2.14100000             -2.14100000              2.14100000
Mg              2.14100000              2.14100000              2.14100000
Mg             -4.28200000             -4.28200000             -3.00000000
Mg             -4.28200000             -0.00000000             -3.00000000
Mg             -4.28200000              4.28200000             -3.00000000
Mg             -0.00000000             -4.28200000             -3.00000000
Mg             -0.00000000             -0.00000000             -3.00000000
Mg             -0.00000000              4.28200000             -3.00000000
Mg              4.28200000             -4.28200000             -3.00000000
Mg              4.28200000             -0.00000000             -3.00000000
Mg              4.28200000              4.28200000             -3.00000000
```

Exercise 7.3: CP2K Input file

(c)(ii) We want to simulate a so-called ”few-cycle” pulse. That can be quantified by $\sigma \cdot \omega_0 = 10\,\mathrm{fs} \cdot 60\,\mathrm{THz} \cdot 2\pi \approx 3.8$, which roughly measures the number of half-cycles (cf. Fig. 1(a)).

```
&GLOBAL
    PROJECT Exc_7
    RUN_TYPE RT_PROPAGATION
&END GLOBAL
&MOTION
    &MD
        ENSEMBLE NVE
        TEMPERATURE 300
        STEPS 1000
        TIMESTEP 0.1
    &END MD
&END MOTION
&FORCE_EVAL
    METHOD QUICKSTEP
    &SUBSYS
        &TOPOLOGY
            &CENTER_COORDINATES
            &END CENTER_COORDINATES
            COORD_FILE_NAME   struc.xyz
            COORD_FILE_FORMAT XYZ
        &END TOPOLOGY
        &CELL
            ABC 10 10 15
            PERIODIC NONE
        &END CELL
```

```
    &KIND Mg
        BASIS_SET ORB DZVP-MOLOPT-SR-GTH-q2
        POTENTIAL GTH-LDA-q2
    &END KIND
&END SUBSYS
&DFT
    &EFIELD
        INTENSITY INDIVIDUAL_INPUT_NEEDED
        POLARISATION 0 0 1
        WAVELENGTH 5000.0
        ENVELOP GAUSSIAN
        &GAUSSIAN_ENV
            SIGMA 10.0
            T0 45.0
        &END GAUSSIAN_ENV
    &END
    &REAL_TIME_PROPAGATION
        MAX_ITER 25
        EPS_ITER 1.0E-9
        MAT_EXP TAYLOR
    &END
    &PRINT
        &MOMENTS
            PERIODIC .FALSE.
        &END
    &END
    BASIS_SET_FILE_NAME BASIS_MOLOPT_UCL
    POTENTIAL_FILE_NAME GTH_POTENTIALS
    &MGRID
        CUTOFF 50
    &END MGRID
    &SCF
        EPS_SCF 1.0E-7
        MAX_SCF 500
        ADDED_MOS -1
        CHOLESKY INVERSE
        &SMEAR ON
            METHOD FERMI_DIRAC
            ELECTRONIC_TEMPERATURE [K] 300
        &END SMEAR
        &MIXING
            METHOD BROYDEN_MIXING
            ALPHA 0.1
            BETA 1.5
            NBROYDEN 8
        &END
```

```
        &END SCF
        &POISSON
            PERIODIC NONE
            POISSON_SOLVER MT
        &END POISSON
        &XC
            &XC_FUNCTIONAL LDA
            &END XC_FUNCTIONAL
        &END XC
    &END DFT
&END FORCE_EVAL
```

Exercise 7.4: Real-time dynamics from TDDFT and comparison to Eq. (1)

(a) cf. (c)

(b) cf. (c)

(c) Fig. 1(a) shows the analytical electric field $E_z(t)$ normalized to 1 and the extracted dipole moments $p_z(t)$ plotted against time. We observe a in-phase behavior with a dependence of $p_z(t)$ on E_0.

Intensity (at.u.)	Electric field peak strength (at.u.)	Maximum dipole strength (at.u.)
10^7	$1.7 \cdot 10^{-5}$	$2.4 \cdot 10^{-2}$
10^9	$1.7 \cdot 10^{-4}$	$2.4 \cdot 10^{-1}$
10^{11}	$1.7 \cdot 10^{-3}$	$2.4 \cdot 10^{0}$
10^{13}	$1.7 \cdot 10^{-2}$	$2.5 \cdot 10^{1}$
$5 \cdot 10^{13}$	$3.8 \cdot 10^{-5}$	$6.2 \cdot 10^{1}$
10^{14}	$5.3 \cdot 10^{-5}$	$8.9 \cdot 10^{1}$

(i) We plot the maximum value of the dipoles p_z against the electric field peak strength E_0 in a double-logarithmic way in Fig. 1(b). As expected, we find the first data points (in the linear response regime) on a line with slope 1 [$\mathbf{p}(t) \propto \mathbf{E}(t')^1$ in Eq. (1)]. The deviation expresses itself by an offset from that line, evidencing higher orders of the dipole moment in $\mathbf{E}(t)^n$

(ii) We plot $p_z(t)/E_0$ in Fig. 1(c). For the smaller E_0 we observe a collapse of the curves to one curve, which shows the applicablity of Eq. (1) for these E_0. For the highest E_0 we observe a deviation, i.e. higher order corrections contribute to the dipole moment. We will discuss the oscillations in the right tail of the dipole moments on the next exercise sheet.

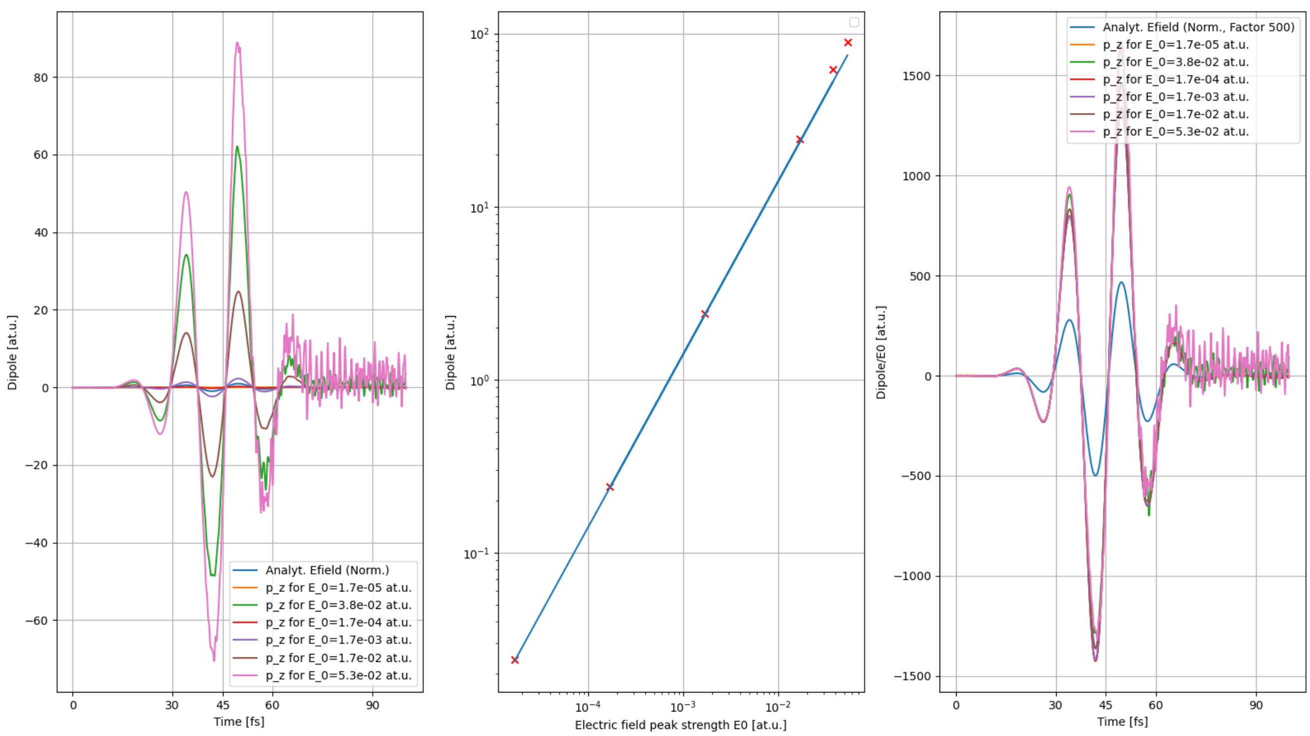

Figure 1: Visualization of the extracted dipoles $\mu_z(t)$ (a) Dipoles $\mu_z(t)$ and normalized electric field $E_z(t)$ against time showing a in-phase behavior with increasing amplitude of $\mu_z(t)$ for increasing E_0. (b) Double-logarithmic plot of maxima of dipoles $\mu_z(t)$ against electric field peak strength E_0. The line is a guide to the eye with linear behavior (Slope=1). The last dipole at $E_0 \approx 1.7 \cdot 10^{-2}$ at.u. shows a clear offset, i.e. deviation, from the linear regime. For even higher E_0, one expects the points to lie on lines with successively increasing slopes (reflecting the increasing order of the expansion of $\mathbf{P}$ in orders of $\mathbf{E}^n$ (c) Dipoles $\mu_z(t)$ normalized by the electric field peak strengths E_0 against time. The dipole for $E_0 \approx 1.7 \cdot 10^{-2}$ at.u. deviates from the other curves, evidencing the deviation from the linear regime. We will discuss oscillations like the one in the right tails of the dipole moments on the next exercise sheet.